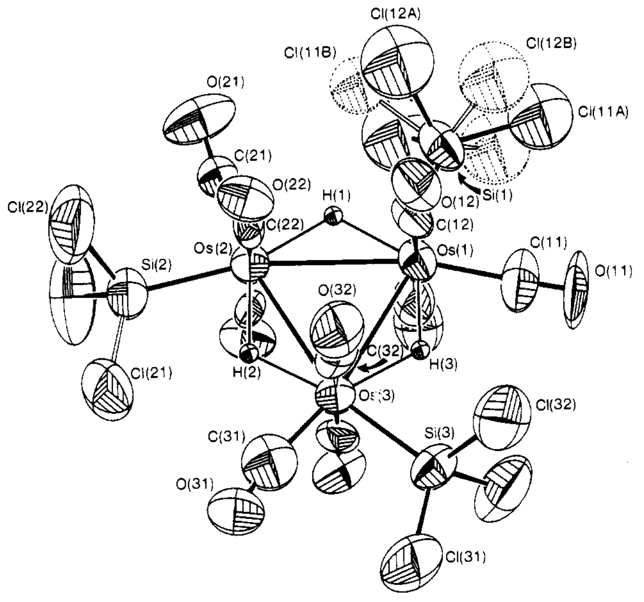

Figure 4. Projection of the $Os_3(\mu\text{-}H)_3(CO)_9(SiCl_3)_3$ molecule, showing the atom-labeling scheme. Both sets of disordered chlorine atoms about Si(1) are shown. Hydrogen atoms are drawn as small spheres at their calculated positions.

present in the same crystal: in one, each methyl group was on the side of the OsHOs bridge, and in the other, each was on the side of the in-plane carbonyl.[8] It is interesting that in the present structure, within an individual molecule, the corresponding in-plane chlorine substituent of one silicon ligand is on the side of the OsHOs bond and in a second it is on the side of the in-plane carbonyl, while in the third, it is disordered between the two positions.

The Os–$SiCl_3$ distances measured in the two structural determinations reported here are not significantly different: 2.377 (3) Å in $Os_3(CO)_{12}(SiCl_3)_2$ and a mean value of 2.383 Å in $Os_3H_3(CO)_9(SiCl_3)_3$. These lengths are slightly shorter than the Os–Si bond lengths in $Os_3H_3(CO)_9(SiMeCl_2)_3$ (mean value 2.410 Å) although the difference is barely significant. This, as discussed previously, may indicate more double-bond character in the Os–$SiCl_3$ linkage.

The osmium–osmium vectors (mean 3.129 Å) found in $Os_3H_3(CO)_9(SiCl_3)_3$ are virtually identical with those found in one conformer of $Os_3H_3(CO)_9(SiMeCl_2)_3$ (3.125 (2) Å); the other conformer had slightly longer Os–Os bonds (3.155 (2) Å). As previously stated, these are among the longest distances determined for such bonds.[8] We are continuing the investigation of silanes with various osmium clusters.

Acknowledgment. We are grateful to the Natural Sciences and Engineering Research Council of Canada for financial support. We also wish to thank Professor W. A. G. Graham and Dr. W. A. Whitla for details of the structure of $Fe(CO)_4(SiCl_3)_2$.

Registry No. A, 84750-97-0; B, 79329-41-2; $Os_3(CO)_{12}(SiMeCl_2)_2$, 84750-98-1; $Os_3(CO)_{12}$, 15696-40-9; Os, 7440-04-2.

Supplementary Material Available: Listings of anisotropic thermal parameters and observed and calculated structure factors for A and B (24 pages). Ordering information is given on any current masthead page.

Contribution from the Departments of Chemistry, Faculty of Science, Osaka City University, Sumiyoshi-ku, Osaka 558, Japan, and Faculty of Science, Tohoku University, Aoba, Aramaki, Sendai 980, Japan

Crystal Structures of V^{IV}, V^{V}, and $V^{IV}V^{V}$ Complexes of the (*S*)-[[1-(2-Pyridyl)ethyl]imino]diacetate Ion. Comparison of the Molecular Structure of the Binuclear Mixed-Valence $V^{IV}V^{V}$ Complex with Those of Constituent V^{IV} and V^{V} Complexes

AKINOBU KOJIMA,[1a] KENICHI OKAZAKI,[1b] SHUN'ICHIRO OOI,*[1a] and KAZUO SAITO[1b]

Received April 28, 1982

The crystal structures of $[VO(S\text{-peida})(H_2O)]\cdot 2H_2O$ (**1**), $Na[V_2O_3(S\text{-peida})_2]\cdot NaClO_4\cdot H_2O$ (**2**), and $Li[VO_2(S\text{-peida})]\cdot 2CH_3OH$ (**3**) have been determined by single-crystal X-ray diffraction (S-peida^{2-}, (*S*)-[[1-(2-pyridyl)ethyl]imino]diacetate). Every vanadium atom in **1**–**3** has an octahedral coordination with a donor atom disposition similar to the others: the axial sites are occupied by O^{2-} and N (tertiary), and there are two O (OOC), one N (pyridine), and one L (L = H_2O in **1**; L = O^{2-} in **2** and **3**) in the equatorial sites. The two coordination octahedra in the mixed-valence binuclear $[V_2O_3(S\text{-peida})_2]^-$ are linked together by sharing the equatorial O^{2-} (O_b) ligand. The $O{=}V_A{-}O_b{-}V_B{=}O$ segment in the dimer has an approximate trans-planar structure ($V{-}O_b{-}V$ = 179.5 (3)°; the torsion angle between the two V=O bonds is 164.3 (2)°). The $V_A{-}O_b$ bond (1.875 (4) Å) differs significantly from the $V_B{-}O_b$ bond (1.763 (4) Å) in length, and furthermore, the volumes of the coordination octahedra around V_A and V_B are close to those of **1** (V^{IV}) and **3** (V^{V}), respectively: i.e., V_A and V_B are inequivalent. These structural features indicate that the mixed-valence dimer should be classified as a class II ion; however, the reflectance spectrum of **2** in the 9000–20 000-cm^{-1} region resembles that of $(NH_4)_3[V_2O_3(nta)_2]\cdot 3H_2O$, in which the anion is known to be a class III ion (nta^{3-} = nitrilotriacetate). Crystal data: **1**, space group $P2_1$, a = 7.707 (3) Å, b = 11.608 (3) Å, c = 8.802 (6) Å, β = 91.84 (3)°, Z = 2; **2**, space group $P2_1$, a = 12.680 (5) Å, b = 15.273 (6) Å, c = 7.856 (3) Å, β = 98.25 (6)°, Z = 2; **3**, space group $P2_12_12_1$, a = 19.387 (2) Å, b = 10.259 (1) Å, c = 8.645 (1) Å, Z = 4. The structures were refined by least squares to R = 0.041, 0.040, and 0.034 for **1**, **2**, and **3**, respectively, with 2013, 2971, and 1871 reflections [$F_o^2 > 3\sigma(F_o^2)$].

Introduction

Coordination chemistry of early transition metals has been drawing increasing attention of chemists, but available structural data are much more limited as compared with those of the other transition elements. During the kinetic study of oxovanadium(IV) complexes we have found the new mixed-valence complex $[V_2O_3(nta)_2]^{3-}$ (nta^{3-} = nitrilotriacetate), in which the two V atoms are linked linearly with the oxide.[2] We

---

[1] (a) Osaka City University. (b) Tohoku University.

[2] Nishizawa, M.; Hirotsu, K.; Ooi, S.; Saito, K. *J. Chem. Soc., Chem. Commun.* **1979**, 771.

0020-1669/83/1322-1168$01.50/0

Table I. Crystal Data and Experimental Details

compd	[VO(*S*-peida)(H_2O)]· $2H_2O$	Na[V_2O_3(*S*-peida)$_2$]· $NaClO_4 \cdot H_2O$	Li[VO_2(*S*-peida)]· $2CH_3OH$
color	blue	dark blue	yellow
formula	$VC_{11}H_{18}N_2O_8$	$V_2C_{22}H_{26}N_4O_{16}ClNa_2$	$VC_{13}H_{20}N_2O_8Li$
fw	357.09	785.53	390.05
space group	$P2_1$	$P2_1$	$P2_12_12_1$
cell const			
a, Å	7.707 (3)	12.680 (5)	19.387 (2)
b, Å	11.608 (3)	15.273 (6)	10.259 (1)
c, Å	8.802 (6)	7.856 (3)	8.645 (1)
β, deg	91.84 (3)	98.25 (6)	
Z	2	2	4
ρ(obsd), g cm^{-3}	1.51	1.72	
ρ(calcd), g cm^{-3}	1.51	1.73	1.51
cryst dimens, mm^3	0.33 × 0.24 × 0.12	0.35 × 0.24 × 0.21	0.30 × 0.30 × 0.15
μ, cm^{-1}	7.11	8.62	6.58
transmission coeff limits	1.09–1.18	1.17–1.25	
scan mode	ω–2θ	ω	ω–2θ
scan speed, deg s^{-1}	0.025	0.033	0.025
scan range in ω, deg	1.00	1.40	$0.9 + 0.3 \tan \theta$
bkgd estimation at each end of the scan, s	half of scan time	20	20
$2\theta_{max}$, deg	60.0	55.0	55.0
unique data measd	2123	3615	2306
obsd reflectns used [$F_o^2 > 3\sigma(F_o^2)$]	2013	2971	1871
R	0.041	0.040	0.034
$R_w = [\Sigma w\Delta^2/\Sigma wF_o^2]^{1/2}$	0.042	0.049	0.040

now succeeded in preparing new optically active complexes of V^{IV}, $V^{IV}V^{V}$ and V^{V} by use of (*S*)-[[1-(2-pyridyl)ethyl]imino]diacetate (*S*-peida^{2-}). This paper deals with the detailed description of X-ray structures of [V^{IV}O(*S*-peida)(H_2O)]·$2H_2O$ (**1**), Na[$V^{IV}V^{V}O_3$(*S*-peida)$_2$]·$NaClO_4 \cdot H_2O$ (**2**), and Li[$V^{V}O_2$(*S*-peida)]·$2CH_3OH$ (**3**) and discusses characteristic features of the mixed-valence complex in comparison with those of the VO^{2+} and VO_2^+ complexes.

Experimental Section

The preparation of the compound will appear in a separate paper.[3]

X-ray Data Collection. Weissenberg and precession photographs taken with Cu Kα radiation were used for investigating Laue symmetry, space group, approximate unit-cell dimensions, and Miller indices for the bounding surfaces of the crystal. The accurate cell dimensions were determined from the least-squares treatments of 24 (**1**), 22 (**2**), and 44 (**3**) θ values of higher angle reflections ($16° < 2\theta < 30°$) measured on a Philips PW1100 diffractometer by use of Mo Kα radiation (λ = 0.71069 Å). Since compound **3** is very hygroscopic, the crystal specimen was sealed within a thin-walled Lindemann glass capillary for use. Crystal data are given in Table I. Intensities were measured on the diffractometer using graphite-monochromated Mo Kα radiation at room temperature (Table I). Stationary-crystal, stationary-counter background counts were measured at each end of the scan. For every crystal the intensities of three standard reflections (200, 020, 002 for **1**; 200, 020, 001 for **2**; 600, 060, 002 for **3**) were monitored every 4 h, but they showed no appreciable decay during the data collection. The intensity data were processed by the computer program of Hornstra and Stubbe[4] by use a value of $p = 0.04$. Absorption correction was applied to the data of **1** and **2** by using the program written by Templeton and Templeton.[5]

Solution and Refinement of Structures. The crystal structures were solved by the Patterson–Fourier method. The positional and thermal parameters were refined by a block-diagonal-matrix least-squares method. The minimized function was $\sum w(|F_o| - |F_c|)^2$, where $w = \sigma^2(F_o)^{-1}$. The convergence was attained with R and $R_w = [\sum w(|F_o| - |F_c|)^2/\sum wF_o^2]^{1/2}$ values listed in Table I. Except for H atoms of the methyl group, the H atoms of the complex ion/molecule were located in the idealized positions (C–H = 0.95 Å). They were in the proximity of the peak positions on the difference Fourier map calculated after the refinement of the structure using anisotropic thermal parameters for non-hydrogen atoms. The methyl, methanol, and water hydrogen atoms were located on the peaks revealed on the difference map. These H atoms were included in the least-squares calculation, but their positional and thermal parameters (B = 5.0 $Å^2$) were fixed. No secondary extinction correction was applied. Final difference syntheses for **1**–**3** showed no anomalous features.

Table II. Positional Parameters (×10^4) for [VO(*S*-peida)(H_2O)]·$2H_2O$ (**1**)

atom	x	y	z
V	3084 (1)	0	4893 (1)
O(1)	3050 (6)	2748 (3)	2099 (3)
O(2)	3395 (3)	1036 (2)	3141 (3)
O(3)	593 (3)	−134 (3)	4167 (3)
O(4)	−2002 (3)	673 (3)	3816 (3)
O(5)	5366 (3)	661 (3)	5668 (3)
O(6)	3588 (4)	−1282 (3)	4399 (4)
N(1)	2558 (4)	−279 (2)	7199 (3)
N(2)	1874 (3)	1673 (3)	5747 (3)
C(1)	2517 (6)	−1347 (4)	7794 (5)
C(2)	2227 (7)	−1531 (4)	9326 (5)
C(3)	1985 (7)	−608 (5)	10231 (5)
C(4)	2011 (6)	500 (4)	9634 (4)
C(5)	2311 (4)	638 (3)	8099 (4)
C(6)	2488 (5)	1807 (3)	7364 (4)
C(7)	2499 (6)	2591 (4)	4745 (4)
C(8)	2995 (5)	2114 (4)	3198 (4)
C(9)	−35 (4)	1537 (3)	5600 (4)
C(10)	−529 (4)	641 (4)	4418 (4)
C(11)	1598 (8)	2786 (4)	8193 (5)
$O_w(1)$	7133 (4)	83 (4)	8086 (3)
$O_w(2)$	3748 (5)	−4289 (4)	9035 (4)

Atomic scattering factors for V^0, Cl^0, Na^+, Li^+, O, N, C, and H, with corrections for anomalous dispersion effects for V^0 and Cl^0, were taken from ref 6. Tables of observed and calculated structure factors and the hydrogen atom coordinates are available as supplementary material. Computational work was carried out by using standard programs.[7]

Spectral Measurement. The reflectance spectra of powder crystals were recorded with a Hitachi 330 spectrometer with a 60ϕ integrating sphere attachment (210–2101).

---

(3) Okazaki, K.; Saito, K. *Bull. Chem. Soc. Jpn.*, in press.

(4) Hornstra, J.; Stubbe, b. "PW1100 Data Processing Program"; Philips Research Laboratories: Eindhoven, Holland.

(5) Templeton, L. K.; Templeton, D. H.; Abstracts, American Crystallographic Association Proceedings, 1973; Series 2, Vol. 1.

(6) "International Tables of X-ray Crystallography"; Kynoch Press: Birmingham, England, 1974; Vol. IV.

(7) "UNICS", Crystallographic Society of Japan, 1969. Johnson, C. K. "ORTEP II", Report ORNL-5138; Oak Ridge National Laboratory: Oak Ridge, TN, 1976.

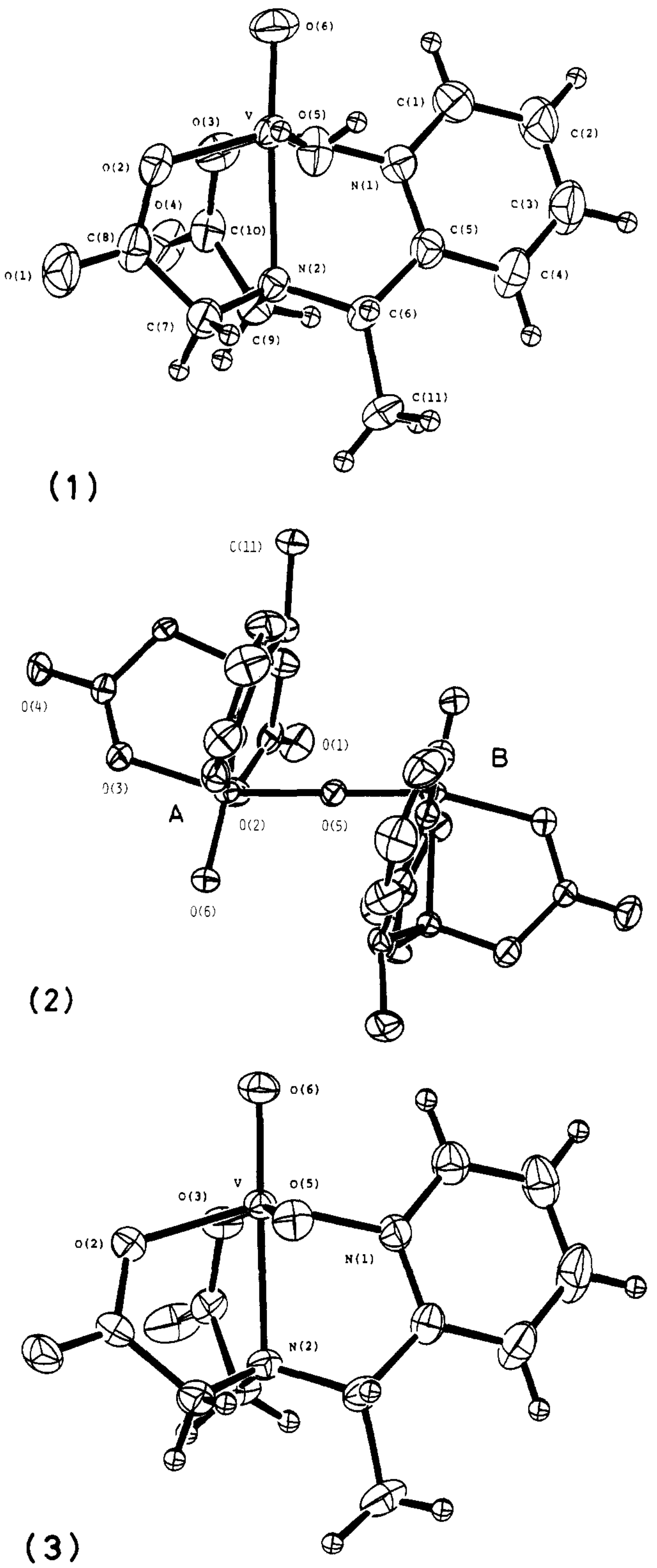

Figure 1. Perspective views of [VO(*S*-peida)(H_2O)] (**1**), [V_2O_3(*S*-peida)$_2$]$^-$ (**2**), and [VO_2(*S*-peida)]$^-$ (**3**). Thermal ellipsoids are drawn at the 50% probability level. Hydrogen atoms are shown by spheres with an arbitrary radius, but those for [V_2O_3(*S*-peida)$_2$]$^-$ are omitted for clarity.

Table III. Positional Parameters ($\times 10^4$) for Na[V_2O_3(*S*-peida)$_2$]·$NaClO_4$·H_2O (**2**)

atom	*x*	*y*	*z*
V_A	1450 (1)	0	1692 (1)
V_B	2575 (1)	1678 (1)	4703 (1)
O(1A)	−11 (3)	−148 (3)	5835 (5)
O(2A)	292 (3)	−121 (3)	3157 (5)
O(3A)	1022 (4)	−1181 (3)	661 (5)
O(4A)	780 (4)	−2602 (3)	1043 (6)
O(6A)	944 (3)	556 (3)	12 (5)
O(5)	2021 (3)	871 (3)	3237 (5)
O(1B)	−528 (4)	1849 (3)	4821 (6)
O(2B)	1211 (3)	1798 (3)	5640 (5)
O(3B)	2988 (3)	2811 (3)	5931 (5)
O(4B)	2477 (3)	4174 (3)	6384 (5)
O(6B)	3355 (4)	1127 (3)	6115 (5)
N(1A)	3011 (4)	−220 (3)	1190 (6)
N(2A)	2183 (3)	−951 (3)	3794 (5)
N(1B)	3616 (4)	1980 (3)	2936 (6)
N(2B)	1696 (4)	2696 (3)	2911 (6)
C(1A)	3322 (5)	34 (5)	−336 (7)
C(2A)	4359 (6)	−87 (5)	−630 (9)
C(3A)	5066 (6)	−471 (5)	582 (10)
C(4A)	4762 (5)	−731 (5)	2140 (9)
C(5A)	3732 (5)	−581 (4)	2409 (7)
C(6A)	3349 (5)	−756 (4)	4115 (7)
C(7A)	1636 (5)	−736 (4)	5293 (7)
C(8A)	564 (5)	−305 (4)	4745 (8)
C(9A)	1974 (5)	−1852 (4)	3153 (8)
C(10A)	1187 (5)	−1891 (4)	1529 (8)
C(11A)	4015 (5)	−1408 (4)	5281 (9)
C(1B)	4636 (5)	1704 (5)	3197 (8)
C(2B)	5272 (6)	1791 (5)	1918 (11)
C(3B)	4849 (7)	2155 (6)	354 (10)
C(4B)	3810 (6)	2431 (5)	115 (8)
C(5B)	3192 (5)	2330 (4)	1421 (7)
C(6B)	2013 (5)	2549 (4)	1172 (7)
C(7B)	571 (5)	2499 (5)	2956 (8)
C(8B)	375 (5)	2015 (4)	4564 (7)
C(9B)	2014 (5)	3572 (4)	3608 (8)
C(10B)	2497 (5)	3538 (4)	5471 (7)
C(11B)	1680 (6)	3287 (5)	−106 (8)
O_w	7958 (6)	1332 (4)	1313 (7)
Na(1)	9758 (2)	1120 (2)	7628 (3)
Na(2)	8462 (2)	467 (2)	3680 (3)
Cl	6854 (1)	804 (1)	6806 (2)
O(1Cl)	6182 (5)	100 (4)	6555 (11)
O(2Cl)	6407 (5)	1529 (4)	7567 (8)
O(3Cl)	7111 (7)	1114 (5)	5219 (9)
O(4Cl)	7893 (6)	590 (5)	7664 (12)

Results

Figure 1 shows perspective views of [VO(*S*-peida)(H_2O)], [V_2O_3(*S*-peida)$_2$]$^-$, and [VO_2(*S*-peida)]$^-$ as well as the atom numbering. Each vanadium atom in these complexes has a coordination geometry similar to the others with the *S*-peida ligand in the same conformation; the tertiary and pyridine nitrogens occupy the axial and equatorial sites of a distorted coordination octahedron, respectively. A common atom numbering was used throughout the three complex molecule/ions except for the O(5), which stands for aqua, bridging oxo (O_b), and oxo ligands in **1**, **2**, and **3**, respectively. Atomic coordinates are given in Tables II–IV.

The vanadium atom in every complex is displaced toward the apical oxo ligand O(6) from the equatorial plane defined by O(2), O(3), O(5), and N(1). The deviation in **1** (0.401 Å) is typical of a 6-coordinate VO^{2+} complex,[8] and that in **3** (0.357 Å) is somewhat larger than those in $(NH_4)_3[VO_2(oxalato)_2]\cdot 2H_2O$ (0.26, 0.29 Å)[9] and [VO(isopropoxo)(8-quinolinato)$_2$] (0.28 Å).[10] In the binuclear ion the displacement of V_A (0.401 Å) is equal to that in **1**, while that of V_B (0.361 Å) is close to the deviation in **3**.

The binuclear ion has an approximate C_2 symmetry, the twofold axis of which passes O_b and is normal to the mean plane of the O=V—O_b—V=O segment. The V–O_b–V bond angle is 179.5°, and thus the arrangement is substantially

---

(8) Ooi, S.; Nishizawa, M.; Matsumoto, K.; Kuroya, H.; Saito, K. *Bull. Chem. Soc. Jpn.* **1979**, *52*, 452 and references therein.

(9) Scheidt, W. R.; Tsai, C.; Hoard, J. L. *J. Am. Chem. Soc.* **1971**, *93*, 3867.

(10) Scheidt, W. R. *Inorg. Chem.* **1973**, *12*, 1758.

Table IV. Positional Parameters ($\times 10^4$) for $Li[VO_2(S\text{-peida})]\cdot 2CH_3OH$ (**3**)

atom	*x*	*y*	*z*
V	−863.0 (3)	−147.1 (5)	1057 (1)
O(1)	496 (1)	−1378 (3)	4193 (3)
O(2)	−449 (1)	−572 (2)	3102 (3)
O(3)	−1657 (1)	−1502 (2)	1823 (3)
O(4)	−1905 (1)	−3525 (3)	2569 (4)
O(5)	−173 (1)	518 (3)	356 (3)
O(6)	−1409 (1)	1061 (2)	1348 (3)
N(1)	−1203 (1)	−717 (3)	−1156 (4)
N(2)	−404 (1)	−2150 (3)	677 (3)
C(1)	−1733 (2)	−120 (4)	−1881 (4)
C(2)	−1920 (2)	−440 (5)	−3376 (5)
C(3)	−1553 (2)	−1386 (5)	−4147 (5)
C(4)	−1011 (2)	−2019 (5)	−3400 (5)
C(5)	−849 (2)	−1667 (4)	−1899 (4)
C(6)	−231 (2)	−2200 (3)	−1017 (5)
C(7)	225 (2)	−2077 (4)	1642 (5)
C(8)	88 (2)	−1316 (3)	3105 (5)
C(9)	−871 (2)	−3197 (3)	1192 (5)
C(10)	−1531 (2)	−2705 (4)	1909 (4)
C(11)	48 (2)	−3505 (5)	−1573 (5)
O(Me1)	1880 (2)	−1159 (3)	2493 (5)
O(Me2)	1850 (1)	−1701 (3)	−3882 (4)
C(Me1)	2293 (3)	−1627 (5)	1321 (7)
C(Me2)	1452 (3)	−1298 (8)	−2675 (7)
Li	1436 (4)	−2101 (7)	4150 (8)

Table V. Bond Lengths (Å)

	$[VO(S\text{-peida})\cdot(H_2O)]$	$[V_2O_3(S\text{-peida})_2]^-$ A	B	$[VO_2(S\text{-peida})]^-$
V-O(6)	1.602 (3)	1.622 (4)	1.613 (4)	1.649 (2)
V-O(5)	2.018 (3)	1.875 (4)	1.763 (4)	1.619 (2)
V-O(3)	2.010 (2)	2.019 (4)	2.013 (4)	2.177 (2)
V-O(2)	1.977 (3)	2.000 (4)	1.983 (4)	1.990 (3)
V-N(1)	2.108 (3)	2.100 (5)	2.099 (5)	2.106 (3)
V-N(2)	2.292 (3)	2.293 (4)	2.278 (4)	2.263 (3)
N(1)-C(5)	1.344 (5)	1.344 (7)	1.345 (7)	1.353 (5)
C(5)-C(6)	1.511 (5)	1.514 (8)	1.516 (8)	1.522 (5)
N(2)-C(6)	1.493 (4)	1.494 (7)	1.496 (7)	1.503 (5)
C(6)-C(11)	1.525 (6)	1.524 (8)	1.528 (8)	1.523 (6)
O(2)-C(8)	1.289 (5)	1.277 (7)	1.300 (7)	1.290 (4)
C(7)-C(8)	1.530 (5)	1.516 (8)	1.515 (9)	1.510 (5)
N(2)-C(7)	1.474 (5)	1.487 (7)	1.464 (7)	1.480 (5)
O(1)-C(8)	1.218 (5)	1.225 (8)	1.218 (7)	1.231 (5)
O(3)-C(10)	1.273 (5)	1.282 (7)	1.298 (7)	1.261 (4)
C(9)-C(10)	1.511 (5)	1.504 (8)	1.504 (8)	1.509 (5)
N(2)-C(9)	1.482 (4)	1.477 (7)	1.480 (7)	1.472 (5)
O(4)-C(10)	1.238 (8)	1.238 (8)	1.210 (7)	1.249 (5)
N(1)-C(1)	1.347 (5)	1.371 (8)	1.348 (8)	1.351 (5)
C(1)-C(2)	1.390 (6)	1.380 (10)	1.382 (11)	1.382 (6)
C(2)-C(3)	1.352 (7)	1.345 (10)	1.385 (11)	1.376 (7)
C(3)-C(4)	1.389 (7)	1.393 (11)	1.370 (11)	1.393 (6)
C(4)-C(5)	1.388 (5)	1.372 (9)	1.386 (10)	1.384 (6)

linear. $O{=}V{-}O_b{-}V{=}O$ deviates slightly from the complete trans-planar structure, from which the $V_B{=}O$ bond is rotated clockwise about the $V_A \rightarrow V_B$ vector by 15.7 (2)°.

The O(3)-V-N(2)-C(9) segment in **3** is planar, the N(2)-C(6) and N(2)-C(7) bonds being disposed symmetrically with respect to the mean plane of this segment. This is not the case for the molecule in **1**. The

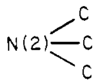

portion is rotated clockwise about the V→N(2) vector; the O(3)-V-N(2)-C(9) torsion angle is 13.4 (2)°. Such a clockwise rotation is also observed in the A and B halves in **2**, but the torsion angles are very small as compared with those in **1** (3.0 (4) and 4.9 (4)° in the A and B halves, respectively).

Interatomic distances and bond angles are listed in Tables V and VI. The V=O length in **1** is comparable to those in $[VO(pmida)(H_2O)]$ ($pmida^{2-}$ = [(2-pyridylmethyl)imino]diacetate) and other VO^{2+} complexes.[8] The axial V=O bond in **3** is 0.030 Å longer than the equatorial one, but these bond lengths are not much different from those in $(NH_4)_3[VO_2(oxalato)_2]\cdot 2H_2O$ (1.635 (2), 1.648 (2) Å)[9] and $NH_4[VO_2(edtaH_2)]\cdot 3H_2O$ (1.623 (2), 1.657 (2) Å).[11] The V=O distance in the binuclear mixed-valence complex is rather close to that in a usual VO^{2+} complex[8] compared to the mean V=O distance in VO_2^+ complexes.[9,11,12] The V=O group is known to give a remarkable trans influence. In $Na_2[(VO)_2(ttha)]\cdot 10H_2O$ ($ttha^{6-}$ = triethylenetetraminehexaacetate), it was found that the trans influence makes the axial V-N(tertiary) bond 0.131 Å longer than the equatorial one.[13] The axial V-N(2) distance in **1** agrees well with that in the ttha complex (2.294 (7) Å) and hence must be under the influence of the apical oxo ligand.

The $V{-}OH_2$ distance in **1** is in agreement with those in the pmida complex (2.02 (1) Å),[8] $VOSO_4\cdot 5H_2O$ (2.006 (1)–2.019 (2) Å),[14] and $(NH_4)_2[VO(oxalato)_2(H_2O)]\cdot H_2O$ (2.033(3) Å).[15] The $V_A{-}O_b$ and $V_B{-}O_b$ distances in the dimer differ from each other, and the difference is significant in view of their esd's. The two vanadium atoms are thus inequivalent in the dimer. However, the mean value of $V{-}O_b$ lengths (1.819 Å) agrees with that in $(NH_4)_3[V_2O_3(nta)_2]\cdot 3H_2O$ (1.810 (1) Å).[2] The mean $V{-}O_b$ distance is fairly longer than the equatorial $V^V{=}O$ distance in **3** and the $V^V{=}O$(isopropoxo) length (1.774 (2) Å) in the 8-quinolinato complex[10] but considerably shorter than V^V-O(OOC), V^{IV}-O(OOC), and $V^{IV}{-}OH_2$ distances.[8-15] The V-N(1) length agrees well with that in the pmida complex (2.11 (1) Å) and that in the 5-coordinate VO(salpn) (2.11 (1) Å)[16] but is slightly shorter than the equatorial V-N(sp^3) bond length in the ttha complex.[13] The V-O(3)(OOC) bond in **3** is considerably longer than the V-O(2) bond owing to the trans influence of the in-plane oxo ligand O(5). The V_A-O(3) and V_B-O(3) bonds in **2** are 0.019 and 0.030 Å longer than the V_A-O(2) and V_B-O(2) bonds, respectively. This should be ascribed to the trans influence of O_b, though the extent is much less pronounced in comparison with that of the VO_2^+ complex in **3**.

The O=V=O angle in VO_2^+ complexes usually ranges from 103.5 to 107.5° and that in **3** lies within this range. In the $O{=}V{-}L_{eq}$ type angle (L_{eq} = donor atom in the equatorial site), the O(6)=V—O(5) and O(6)=V—O(2) angles are always larger than the O(6)=V—O(3) and O(6)=V—N(1) angles, respectively, throughout the three complexes. This indicates that the axial V=O(6) bond tilts toward the O(3)⋯N(1) edge in these three, irrespective of the environmental differences. The same tilt was also found in the pmida chelate,[8] which is structurally very similar to $[VO(S\text{-peida})(H_2O)]$, except that it has no methyl substituent. Such a tilt of the V=O bond in **1**–**3** as well as the pmida chelate means that the chelation of either ligand displaces the coordination sites in the idealized skeleton for the VO_2^+ or VO^{2+} complex, owing to the strain characteristics of the pmida frame. Thus the chelation gives rise to a slant of the mean equatorial plane

---

(11) Scheidt, W. R.; Collins, D. M.; Hoard, J. L. *J. Am. Chem. Soc.* **1971**, *93*, 3873.

(12) Scheidt, W. R.; Countryman, R.; Hoard, J. L. *J. Am. Chem. Soc.* **1971**, *93*, 3878.

(13) Fallon, G. D.; Gatehouse, B. M. *Acta Crystallogr., Sect. B* **1976**, *B32*, 71.

(14) Tachez, M.; Theobald, F.; Watson, K. J.; Mercier, R. *Acta Crystallogr., Sect. B* **1979**, *B35*, 1545.

(15) Oughtred, R. E.; Raper, E. S.; Shearer, H. M. M. *Acta Crystallogr., Sect. B* **1976**, *B32*, 82.

(16) Mathew, M.; Carty, A. J.; Palenik, G. J. *J. Am. Chem. Soc.* **1970**, *92*, 3197.

Table VI. Bond Angles (deg)

		$[V_2O_3(S\text{-peida})_2]^-$		
	$[VO(S\text{-peida})(H_2O)]$	A	B	$[VO_2(S\text{-peida})]^-$
O(6)-V-O(5)	103.2 (1)	103.1 (2)	103.4 (2)	105.7 (1)
O(6)-V-O(3)	94.5 (1)	95.1 (2)	91.6 (2)	88.8 (1)
O(6)-V-O(2)	108.5 (1)	106.2 (2)	105.9 (2)	106.7 (1)
O(6)-V-N(1)	100.1 (1)	101.8 (2)	100.8 (2)	98.4 (1)
O(6)-V-N(2)	168.9 (1)	171.7 (2)	168.0 (2)	163.1 (1)
N(2)-V-O(5)	85.8 (1)	84.5 (2)	87.7 (2)	90.2 (1)
N(2)-V-O(3)	77.0 (1)	77.4 (2)	77.3 (2)	75.1 (1)
N(2)-V-O(2)	78.5 (1)	77.4 (2)	77.9 (2)	76.8 (1)
N(2)-V-N(1)	73.8 (1)	74.8 (2)	74.9 (2)	74.9 (1)
O(5)-V-O(3)	161.9 (1)	161.8 (2)	165.0 (2)	165.2 (1)
O(2)-V-N(1)	151.3 (1)	152.0 (2)	152.9 (2)	150.7 (1)
V-N(1)-C(5)	118.8 (2)	119.7 (4)	117.6 (4)	118.2 (2)
N(1)-C(5)-C(6)	116.3 (3)	115.6 (5)	117.6 (5)	114.8 (3)
C(5)-C(6)-N(2)	106.5 (3)	108.7 (4)	107.7 (4)	107.5 (3)
C(5)-C(6)-C(11)	114.6 (3)	115.3 (5)	114.9 (5)	116.0 (3)
N(2)-C(6)-C(11)	113.6 (3)	114.9 (5)	113.9 (5)	114.7 (3)
V-N(2)-C(6)	106.3 (2)	106.6 (3)	106.9 (3)	105.1 (2)
V-O(2)-C(8)	121.6 (2)	117.7 (4)	117.1 (4)	117.2 (2)
O(2)-C(8)-C(7)	116.9 (3)	118.6 (5)	116.8 (5)	116.5 (3)
O(2)-C(8)-O(1)	122.7 (4)	122.3 (5)	122.5 (5)	123.5 (3)
C(7)-C(8)-O(1)	120.3 (4)	119.0 (5)	120.7 (5)	120.0 (3)
C(8)-C(7)-N(2)	111.5 (3)	111.8 (5)	113.4 (4)	110.7 (3)
V-N(2)-C(7)	105.8 (2)	104.1 (3)	103.7 (3)	101.3 (2)
V-O(3)-C(10)	122.5 (2)	121.9 (4)	121.3 (3)	120.4 (2)
O(3)-C(10)-C(9)	116.7 (3)	117.1 (5)	114.4 (5)	117.9 (3)
O(3)-C(10)-O(4)	124.4 (4)	123.3 (5)	124.8 (5)	125.0 (3)
C(9)-C(10)-O(4)	118.8 (3)	119.5 (5)	120.5 (5)	117.1 (3)
C(10)-C(9)-N(2)	111.2 (3)	113.0 (5)	112.3 (5)	113.7 (3)
V-N(2)-C(9)	107.1 (1)	108.1 (3)	107.8 (3)	112.2 (2)
C(1)-N(1)-C(5)	119.6 (3)	119.2 (5)	120.8 (5)	119.5 (3)
N(1)-C(1)-C(2)	121.7 (4)	120.6 (5)	120.5 (6)	121.7 (4)
C(1)-C(2)-C(3)	118.6 (5)	119.6 (7)	119.4 (7)	119.0 (4)
C(2)-C(3)-C(4)	120.5 (4)	120.4 (7)	119.1 (7)	119.6 (4)
C(3)-C(4)-C(5)	118.7 (4)	118.5 (6)	120.0 (6)	118.9 (4)
C(4)-C(5)-N(1)	120.9 (4)	121.6 (6)	120.1 (6)	121.2 (4)
V_A-O(5)-V_B		179.5 (3)		

against that in the idealized skeleton in which the V═O bond is probably perpendicular to the equatorial plane.

The corresponding bond lengths and angles of the peida ligand themselves in **1**–**3** are almost in agreement with one another. The sole exception is that the C(10)–O(3) and C(10)–O(4) distances of the COO^- group trans to O(5) in **3** are not much different from each other, in contrast to the significant difference between the C(8)–O(2) and C(8)–O(1) distances of the COO^- cis to the oxo ligand in **3** and **2**. Similar trends are observed in $(NH_4)_3[VO_2(oxalato)_2]\cdot 2H_2O$[9] and $(NH_4)_2[VO(oxalato)_2(H_2O)]\cdot H_2O$.[15] The differences in the two C–O bonds in these complexes are in the 0.021–0.024 Å range when the COO^- is trans to the oxo ligand, whereas they are in the 0.046–0.070 Å range for the COO^- cis to the oxo ligand. Strong trans influence of the V═O seems to diminish the polarization of the trans COO^- group.

Crystal Packing. Short contacts and hydrogen bonds in **1**–**3** are summarized in Table VII. In **1**, all the H atoms of $H_2O_w(1)$ and ligating $H_2O(5)$ participate in O—H···O(O═C or OH_2) hydrogen bonding, while one of the H atoms of $H_2O_w(2)$ does not. In **3**, all the MeOH molecules are linked to the O(O═C) atom of the COO^- group trans to the O(5) via the OH group (H···O(4)···H = 105°), while the Li^+ ion approaches the O(O═C) of the COO^- cis to the O(5) at a distance 1.968 Å. The Li^+ ion is surrounded tetrahedrally by two O atoms of the MeOH molecules, the O(1)(O═C) of the "cis COO^-", and the O(6)(O═V) of the adjacent complex ion at the equivalent position ($-x$, $y - {}^1/_2$, ${}^1/_2 - z$), the Li^+···O distances ranging 1.926–1.968 Å.

(**2**) The halves of the dimer are very similar to each other in structure, but the surrounding of the A moiety is somewhat different from that of the B moiety as described below. Both glycinato rings ($\overline{\text{V–N–CH}_2\text{–COO}}$) are located in one side of the mean plane of O═V—O_b—V═O, while solely pyridine groups are present in the other side. Five Na^+ ions are dis-

Table VII. Short Contacts

compd	A···B	dist, Å	position of B
1	$O_w(1)$···H(1-O5)	1.93	x, y, z
	$O_w(2)$···H(2-O_w1)	2.23	$1 - x, -{}^1/_2 + y, 2 - z$
	O(4)···H(2-O5)	1.79	$-1 + x, y, z$
	O(4)···H(1-O_w2)	2.04	$-x, {}^1/_2 + y, 1 - z$
	O(1)···H(1-O_w1)	1.93	$1 - x, {}^1/_2 + y, 1 - z$
2	Na(1)···O(4Cl)	2.503 (8)	x, y, z
	O(6A)	2.389 (5)	$1 + x, y, 1 + z$
	O(1A)	2.437 (6)	$1 + x, y, z$
	O(3A)	2.353 (5)	$1 - x, {}^1/_2 + y, 1 - z$
	O(1B)	2.444 (6)	$1 + x, y, z$
	O(2B)	2.787 (5)	$1 + x, y, z$
	Na(2)···O(3Cl)	2.459 (9)	x, y, z
	O_w	2.296 (6)	x, y, z
	O(1A)	2.549 (6)	$1 + x, y, z$
	O(2A)	2.566 (5)	$1 + x, y, z$
	O(1B)	2.570 (6)	$1 + x, y, z$
	O(4B)	2.294 (6)	$1 + x, y, z$
	O(4A)···H(2-O_w)	2.99	$1 - x, -{}^1/_2 + y, -z$
	O(2Cl)···H(2-O_w)	2.51	$x, y, 1 + z$
	O(4Cl)···H(2-O_w)	2.14	$x, y, 1 + z$
3	Li···O(1)	1.968 (7)	x, y, z
	O(Me1)	1.929 (8)	x, y, z
	O(Me2)	1.926 (8)	$x, y, 1 + z$
	O(6)	1.935 (7)	$-x, {}^1/_2 + y, {}^1/_2 - z$
	O(4)···H(OMe1)	1.75	$-x, -{}^1/_2 + y, {}^1/_2 - z$
	H(OMe2)	1.82	$-{}^1/_2 + x, -{}^1/_2 - y, -z$

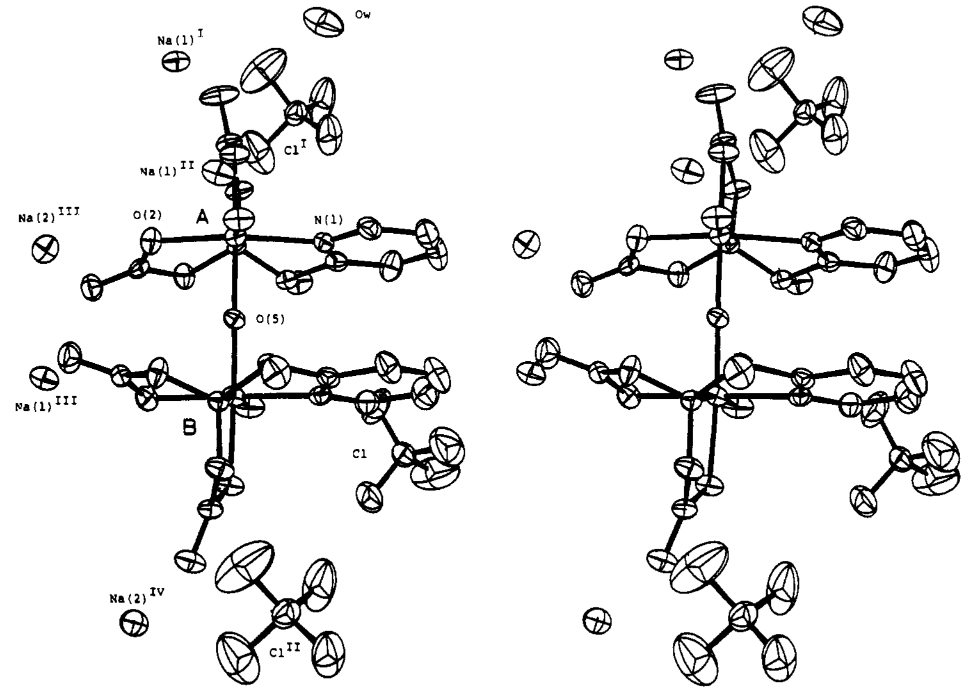

Figure 2. Stereoview showing the evironment of $[V_2O_3(S\text{-peida})_2]^-$. Roman numerical superscripts for Na^+ and Cl (in ClO_4^-) refer to the following equivalent positions: (I) $1 - x, y - {}^1/_2, 1 - z$, (II) $x - 1, y, z - 1$, (III) $x - 1, y, z$, and (IV) $1 - x, {}^1/_2 + y, 1 - z$ for Na^+; (I) $1 - x, y - {}^1/_2, 1 - z$ and (II) $1 - x, {}^1/_2 + y, 1 - z$ for Cl.

tributed in the glycinato side and are in contact with the carboxylato O and O(6A) atoms. On the other hand, three ClO_4^- anions are located in the pyridine side (Figure 2). The $Na^+\cdots O(OOC)$ distances are in the 2.294–2.787 Å range, which is normal for $Na^+\cdots O$ contacts. The Cl^I atom is 6.862 (2) Å away from the V_A atom. Cl and Cl^{II} are 5.827 (2) and 6.453 Å from the V_B, respectively. Of the five Na^+ cations, three are close to the A half, and two of the three ClO_4^- anions are located in the B side. The cation and anion distribution around the dimer indicates that the A moiety has more negative charge than the B moiety.

Discussion

As described above, the two vanadium atoms are inequivalent in the mixed-valence dimer. Some of the bond lengths and angles around V_A differ significantly from those around V_B. With the aim of comparing the coordination sites between V_A and V_B, the volumes of the coordination octahedra around the vanadium atoms were calculated to be 9.95 (2) and 9.58 (2) Å^3 for the A and B octahedra, respectively. The corresponding volumes are 10.01 (2) and 9.62 (2) Å^3 for $[VO(S\text{-peida})(H_2O)]$ and $[VO_2(S\text{-peida})]^-$, respectively. The volumes of the A and B octahedra are thus close to those of the V(IV) and V(V) complexes, respectively. Furthermore, the deviation of V_A from the [N(1A),O(2A),O(3A),O(5)] plane is equal to that of the V(IV) atom from the equatorial plane of $[VO(S\text{-peida})(H_2O)]$, and that of V_B from the [N(1B),O(2B),O(3B),O(5)] plane is rather close to that of the V(V) atom in $[VO_2(S\text{-peida})]^-$. These structural features as well as the cation and anion distribution around the dimer strongly indicate that V_A and V_B are quadri- and quinquevalent in character, respectively. Hence, the mixed-valence dimer can be regarded as the class II ion of Robin and Day's classification.[17] An attempt was made to investigate the XPS's of **1**–**3** to obtain direct evidence for the oxidation states of the vanadium atoms in the dimer. However, these compounds decomposed under the experimental conditions for XPS measurement (the colors of **1**–**3** changed to brown).

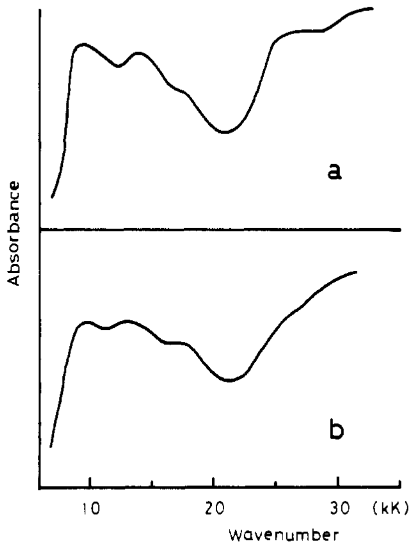

Figure 3. Reflectance spectra of $Na[V_2O_3(S\text{-peida})_2]\cdot NaClO_4\cdot H_2O$ (a) and $(NH_4)_3[V_2O_3(nta)_2]\cdot 3H_2O$ (b).

The reflectance spectrum of **2** shows peaks at 9400, 13 900, 17 400, and 26 800 cm^{-1} (Figure 3) and resembles its solution spectrum [10 200, (ϵ = 1200), 13 600 (940), 17 700 cm^{-1} (470)].[3] There seems no large variation between the dimer structure in the solid state and that in solution. The absorption bands in 12 000–30 000-cm^{-1} region are very similar in energy to those of **1** at 13 200 (ϵ = 27.4), 17 700 (16.4), and 28 200 cm^{-1} (357), which are assigned to $d_{xy} \rightarrow d_{xz}, d_{yz}$, $d_{xy} \rightarrow d_{x^2-y^2}$, and $d_{xy} \rightarrow d_{z^2}$ transitions, respectively.[3] However, the absorption of the dimer is much enhanced in comparison with that of **1**. The reflectance spectrum of $(NH_4)_3[V_2O_3(nta)_2]\cdot 3H_2O$ is also presented in Figure 3. The nta complex has a structure similar to $[V_2O_3[S\text{-peida})_2]^-$, but the two vanadium atoms are reckoned to be equivalent at ambient temperature on the bases of solution ESR and crystallography.[2] It has a crystallographically imposed center of symmetry, and the $V{-}O_b{-}V$ bond is completely linear and symmetric, but its

---

[17] Robin, M.; Day, P. *Adv. Inorg. Chem. Radiochem.* **1967**, *10*, 247.

symmetry can be approximated virtually to C_{2h}. The reflectance spectrum of the *S*-peida dimer resembles that of the nta dimer in 9000–20 000-cm^{-1} region. This indicates that these complexes have similar electronic structures, although the dimers in the former and latter are regarded crystallographically as class II and class III ions, respectively. The absorption around 10 000 cm^{-1} is characteristic of the mixed-valence dimer. No such band is found in the uninuclear VO^{2+} and VO_2^+ complexes.

The linearity and bond length in V–O$_b$–V in these dimers indicate the presence of a multiple bonding. In the symmetric C_{2h} dimer, the bonding in V–O$_b$–V may be qualitatively described as follows. The p_y (O$_b$) orbital participates in σ bonding along with the $d_{x^2-y^2}$ orbitals of two vanadium atoms (the y axis parallels the V–O$_b$–V bond). Both the p_x and p_z orbitals of O$_b$ are capable of coupling with metal d_{xy} and d_{yz} to give π bonds, but the d_{xy}–p_x–d_{xy} set is energetically more favorable than the d_{yz}–p_z–d_{yz} set. The bonding orbital in the former set (a_u) accommodates two π electrons. The single d electron in this system may occupy the nonbonding b_g orbital mainly composed of the metal d_{xy} orbitals.

The orbital of the nonsymmetric dimer corresponding to the nonbonding orbital in the symmetric dimer mainly consists of the d_{xy} orbital of the V_A atom, since the d electron is virtually localized at the V_A center as described above. The polarized charge distribution around the dimer seems to cause the localization of the electron. The absorption at ~10 000 cm^{-1} in the symmetric dimer may arise from an electronic excitation from the nonbonding to antibonding (a_u*) orbital. The antibonding orbital of the nonsymmetric dimer must have a greater contribution from the d_{xy} orbital of V_B than that of V_A, and in this sense the lowest energy absorption in the solid state may be regarded as a kind of intervalence-transfer transition.

Registry No. **1**, 81898-97-7; **2**, 84863-66-1; **3**, 84894-05-3.

Supplementary Material Available: Tables of observed and calculated structure factor amplitudes, hydrogen atom coordinates, and anisotropic thermal parameters (14 pages). Ordering information is given on any current masthead page.

Contribution from the Chemistry Division,
Oak Ridge National Laboratory, Oak Ridge, Tennessee 37830

Solvent-Extraction Complexes of the Uranyl Ion. 2. Crystal and Molecular Structures of *catena*-Bis(μ-di-*n*-butyl phosphato-*O*,*O'*)dioxouranium(VI) and Bis(μ-di-*n*-butyl phosphato-*O*,*O'*)bis[(nitrato)(tri-*n*-butylphosphine oxide)dioxouranium(VI)]

JOHN H. BURNS

Received September 16, 1982

Two complexes of the uranyl ion with organophosphorus extractants have been analyzed by single-crystal X-ray diffraction methods. A polymeric complex, $UO_2[(C_4H_9)_2PO_4]_2$, is formed with dibutylphosphoric acid; and with a mixture of this acid and tributylphosphine oxide a dimeric complex having the composition $\{UO_2[(C_4H_9)_2PO_4][(C_4H_9)_3PO]NO_3\}_2$ is formed. The first of these is triclinic, $P\bar{1}$, with a = 8.402 (6) Å, b = 15.648 (9) Å, c = 5.385 (3) Å, α = 99.46 (4)°, β = 98.51 (4)°, γ = 70.44 (3)°, and Z = 1; the second is also triclinic, $P\bar{1}$, with a = 13.510 (6) Å, b = 13.741 (6) Å, c = 10.055 (4) Å, α = 121.32 (2)°, β = 100.28 (3)°, γ = 80.00 (4)°, and Z = 1 (dimer). In each structure, pairs of linear uranyl ions are bridged by two dibutyl phosphate ions. In one case the bridging is repeated indefinitely to form a polymer, and each uranyl ion has four O atoms about its equator. The other structure is dimeric, and the chain is terminated by NO_3^- ions and phosphine oxide molecules at the equators of the uranyl ions.

Introduction

A variety of organophosphorus compounds when dissolved in organic solvents are effective in extracting U(VI) from acidic aqueous solutions.[1] In the liquid–liquid extraction process usually employed, the UO_2^{2+} ion moves from the aqueous phase to the organic as its aqueous solvation sphere is replaced by organophosphorus ligands to form extraction complexes. The structures of a number of these complexes are being studied in order better to understand the process of extraction. One such structure, previously reported,[2] is that of $UO_2(TBPO)_2(NO_3)_2$, in which TBPO ≡ tri-*n*-butylphosphine oxide. Here the equatorial plane of the UO_2^{2+} ion contains no water but is occupied by two molecules of TBPO and two NO_3^- ions. An analogous arrangement to this also exists in $UO_2L_2(NO_3)_2$ in cases where L = triethyl phosphate,[3] triisobutyl phosphate,[4] and triphenylphosphine oxide.[5]

There is also the interesting question of why certain combinations of reagents are better extractants than either of the components alone (the so-called synergistic effect[6-8]). Hence, in addition to the complex with TBPO mentioned above, a complex with di-*n*-butylphosphoric acid (HDBP) has been studied as well as a complex with a mixture of the two ligands. These latter two uranyl complexes are reported here. From these crystal structure analyses it can be seen how each component combines with the uranyl ion and what the result is of using a mixture of the two.

Experimental Section

Preparation of $UO_2(DBP)_2$. Di-*n*-butylphosphoric acid was obtained from a mixture of mono- and dibutylphosphoric acids (Mobil Chemical Co., Richmond, VA) by dissolving the mixture in benzene and extracting out the monoacid with water. A 1:2 mixture of $UO_2(NO_3)_2\cdot 6H_2O$ and HDBP was heated to about 65 °C until it was liquid; in the process there were an evolution of brown oxides of nitrogen and the formation of tiny droplets of H_2O. The yellow liquid was desiccated over H_2SO_4 and gradually crystallized as a mass of thin plates of $UO_2(DBP)_2$. These bend easily or split into fibers, showing a mechanical property related to their polymeric structure.

Preparation of $UO_2(DBP)(TBPO)NO_3$. A 1:1:2 mixture of $UO_2(NO_3)_2\cdot 6H_2O$, TBPO (Carlisle Chemical Works, Reading, OH),

---

[1] Blake, C. A., Jr.; Baes, C. F., Jr.; Brown, K. B. *Ind. Eng. Chem.* **1958**, *50*, 1763.

[2] Part 1: Burns, J. H. *Inorg. Chem.* **1981**, *20*, 3868.

[3] Fleming, J. E.; Lynton, H. *Chem. Ind.* (*London*) **1960**, 1415.

[4] Burns, J. H.; Brown, G. M., unpublished results.

[5] Alcock, N. W.; Roberts, M. M.; Brown, D. *J. Chem. Soc., Dalton Trans.* **1982**, 25.

[6] Baes, C. F., Jr. *Nucl. Sci. Eng.* **1963**, *16*, 405.

[7] Deane, A. M.; Kennedy, J.; Sammes, P. G. *Chem. Ind.* (*London*) **1960**, 443.

[8] Dyrssen, D.; Kuca, L. *Acta Chem. Scand.* **1960**, *14*, 1945.

0020-1669/83/1322-1174$01.50/0